



ELSEVIER

Automation in Construction xx (2007) xxx – xxx

AUTOMATION IN CONSTRUCTION

www.elsevier.com/locate/autcon

1

2

Cable-suspended robotic contour crafting system

3

Paul Bosscher ^a, Robert L. Williams II ^{a,*}, L. Sebastian Bryson ^b, Daniel Castro-Lacouture ^b

4

^a Department of Mechanical Engineering, Ohio University, Athens, Ohio 45701, United States

5

^b Department of Civil Engineering, Ohio University, Athens, Ohio 45701, United States

6

Accepted 20 February 2007

7

Abstract

8

This article introduces a new concept for a contour crafting construction system. Contour crafting is a relatively new layered fabrication technology that enables automated construction of whole structures. The system proposed here consists of a mobile contour crafting platform driven by a translational cable-suspended robot. The platform includes an extrusion system for laying beads of concrete as well as computer-controlled trowels for forming the beads as they are laid. This system is fully automated and its goal is to construct concrete structures rapidly and economically. The novel attributes of this system potentially enable significant improvements over other proposed contour crafting systems, including better portability, lower cost, and the possibility to build much larger structures. This article presents the kinematics and statics of the proposed system, provides a proof of translation-only motion, and uses the reachable workspace of the robot as well as the corresponding cable tensions to approximate the maximum size structure that can be built using this manipulator.

16

© 2007 Elsevier B.V. All rights reserved.

17

18

Keywords: Contour crafting; Concrete extrusion; Cable-suspended robot; Workspace; Translation-only robot

19

20

1. Introduction

21

Contour crafting (CC) is a layered fabrication technology that has been proposed by Khoshnevis [1,2] for automated construction of civil structures. The aim of this technology is to improve the speed, safety, quality and cost of building construction.

25

Similar to other layered fabrication technologies such as rapid prototyping, stereolithography and solid free-form fabrication, CC uses a computer controlled process to fabricate structures by depositing layers of material, building the structure from the ground up, one layer at a time. However, unlike existing layered fabrication processes, CC is designed for construction of very large scale structures, on the scale of single-family homes up to housing complexes and office buildings. Fig. 1 shows a schematic (from [1]) showing a building being constructed using CC.

34

The CC process involves depositing strips/beads of material (typically a thick concrete/paste type material) using an extrusion process. A nozzle (shown in yellow in Fig. 1) extrudes the material in the desired locations. In the original formulation of this system the x - y - z position of the nozzle is controlled by a Cartesian gantry manipulator. This article will present an alternative manipulator for performing this task.

As the nozzle moves along the walls of the structure the construction material is extruded and troweled using a set of actuated, computer controlled trowels. The use of computer-controlled trowels allows smooth and accurate surfaces to be produced. Fig. 2 shows a close-up of the extrusion/troweling tool in a small-scale prototype CC system developed by Koshnevis (from [1]).

Because of the highly automated nature of CC, it has the potential to significantly increase the speed and decrease the cost of concrete structure construction. This technique also greatly increases design flexibility, as architects would be able to design structures with complex geometries that would be difficult to construct using current concrete construction techniques. In addition to automated deposition of concrete-like materials, the system could be modified to allow automated

* Corresponding author. Tel.: +1 740 593 1096; fax: +1 740 593 0476.

E-mail addresses: bosscher@ohio.edu (P. Bosscher), williar4@ohio.edu (R.L. Williams), bryson@ohio.edu (L.S. Bryson), castro-l@ohio.edu (D. Castro-Lacouture).

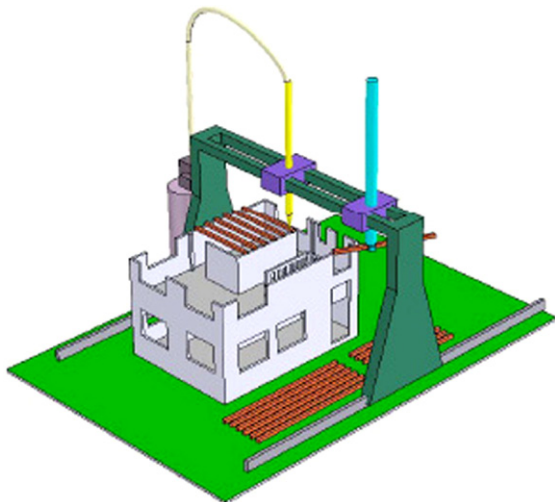


Fig. 1. Construction of a building using contour crafting and a gantry robot system (figure from [1]).

Sections 5 and 6. Proof of translation-only motion of the manipulator is given in Section 7. The workspace of the manipulator is studied in Section 8, including an examination of the cable tensions throughout the workspace. Finally Section 9 presents some conclusions and future work.

2. Cable robots

Cable-driven robots (or cable-suspended robots or tendon-driven robots), referred to here as cable robots, are a type of robotic manipulator that has recently attracted interest for large workspace manipulation tasks. Cable robots are relatively simple in form, with multiple cables attached to a mobile platform or end-effector as illustrated in Fig. 3. The end-effector is manipulated by motors that can extend or retract the cables. In addition to large workspaces, cable robots are relatively inexpensive and are easy to transport, disassemble and reassemble. Cable robots have been used for a variety of applications, including material handling [3–5], haptics [7,8], and many others.

Based on the degree to which the cables determine the pose (position and orientation) of the manipulator, cable robots can be put into one of two categories: fully-constrained and underconstrained. In the fully-constrained case the pose of the end-effector can be completely determined given the current lengths of the cables. Fig. 4 shows an example of a fully-constrained cable robot, the FALCON-7 [3], a small-scale seven-cable high-speed manipulator able to achieve accelerations up to 43 g. Fully constrained cable robots have been designed for applications that require high precision, high speed/acceleration or high stiffness. Underconstrained cable robots have been proposed by the second author and NIST for contour crafting type construction [6]. However, because of the need for large workspace manipulation that has both precise motion and high stiffness, we propose the use of a fully-constrained cable robot for contour crafting.

Several other fully-constrained cable robots exist ([8–10]). However, these manipulators are only practical for small-workspace applications because the required geometry of the cables and end-effector for these manipulators are not intended for large workspaces. For example, implementing the FALCON-7 in Fig. 4 on a large scale would require a very large and cumbersome end-effector rod. In addition, fully constrained

addition of reinforcement materials, plumbing and electrical wiring as the structure is being built (see [1] for more details).

The CC process relies on manipulating the extrusion/troweling nozzle through a very large workspace. Since this manipulation primarily requires only Cartesian motion, a gantry system has been proposed in [1] for performing this motion. However, in [1] it is recognized that building very large structures with a gantry robot requires an extremely large gantry robot, which may be difficult to build and implement. Indeed, such a manipulator would be relatively large and heavy, with massive actuators. It could be cumbersome to transport and deploy at a construction site. In this article an alternative manipulator is presented for performing Cartesian manipulation of a CC platform.

The outline of this article is as follows. First the use of cable robots for CC is motivated in Section 2. In Section 3 a cable robot concept, termed the Cable-Suspended Contour-Crafting Construction (C^4) Robot, is presented for performing CC tasks. The operation of the system is then described in Section 4, followed by a discussion of the robot kinematics and statics in

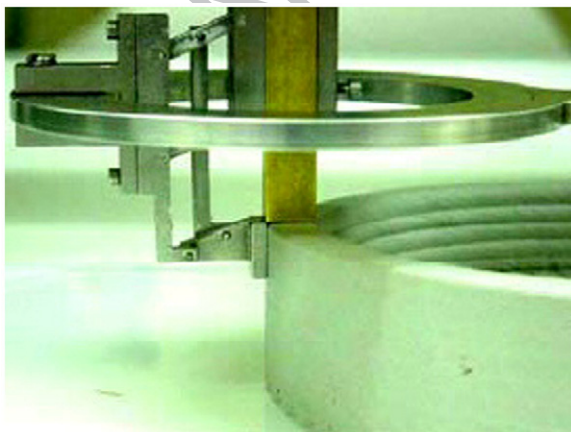


Fig. 2. Prototype of contour crafting system (figure from [1]).

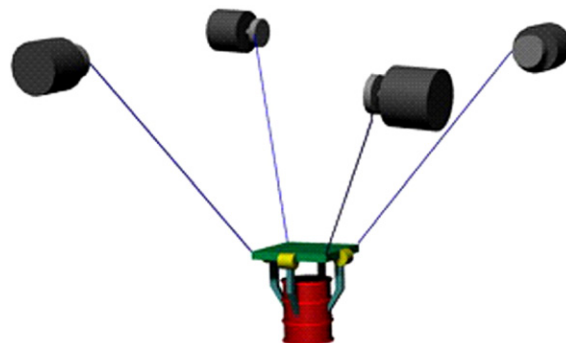


Fig. 3. Example cable robot.

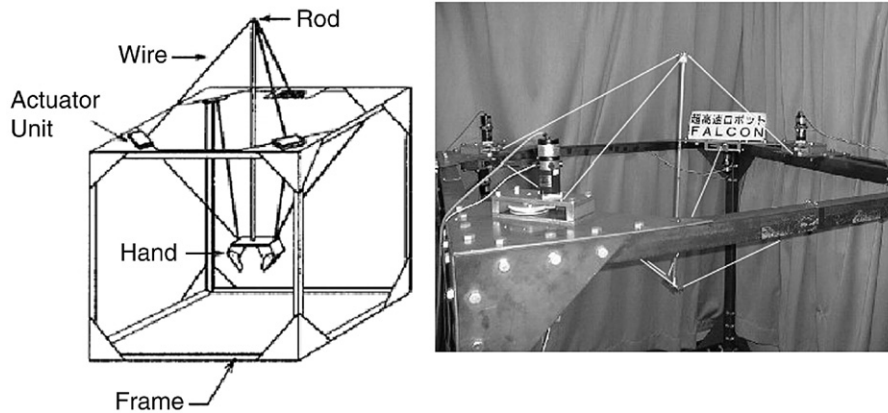


Fig. 4. Falcon-7 (figures from [3]).

118 cable robots often have cable interference issues, particularly
 119 with the cables colliding with nearby objects. The manipulator
 120 presented here is designed to be practical for large workspace
 121 manipulation while avoiding collisions between itself and the
 122 structures being built.

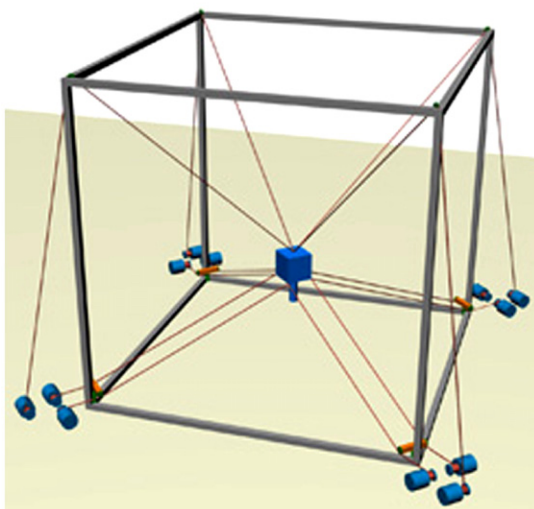
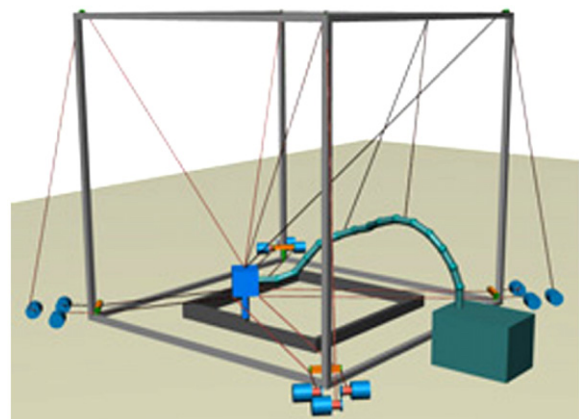
123 3. Contour crafting Cartesian cable robot

124 To perform the task of translation-only manipulation of an
 125 extrusion/construction end-effector through large workspaces
 126 for CC tasks, we are proposing the Contour Crafting Cartesian
 127 Cable Robot, abbreviated as the C^4 robot. The C^4 robot, shown
 128 in Fig. 5, consists of a rigid frame and an end-effector sus-
 129 pended from twelve cables, grouped into four upper cables and
 130 eight lower cables. The eight lower cables are additionally
 131 divided into four pairs of parallel cables. The arrangement of the
 132 cables is derived from a previous cable robot developed by the
 133 first two authors [12] for translation-only motion.

134 The cables are routed through pulleys that are mounted to a
 135 large cube-shaped frame to motors that actuate the lengths of the
 136 cables, which can be located at the base of the frame. The frame
 137 consists of truss-like members that can be easily transported and

assembled at the construction site. The frame must be large
 enough to completely enclose the structure that is being built.
 The pulleys for the lower cables are mounted on horizontal
 crossbars, oriented at an angle of 45° with respect to the adja-
 cent horizontal frame members, where the width of each cross-
 bar is equal to the width of the corresponding side of the end-
 effector. The end-effector includes all of the extrusion and
 troweling tools for performing CC. The concrete is pumped
 from an external storage tank to the end-effector via a flexible
 suspended hose, as shown in Fig. 6.

The function of the upper cables is essentially to support the
 weight of the end-effector, while the lower cables provide the
 required translation-only motion. For each pair of cables, the
 two cables are controlled such that they have the same length
 (this can be easily accomplished by reeling in each pair of
 cables with a single motor). As a result, a parallelogram is
 formed by each pair of cables and the corresponding crossbar
 and the edge of the end-effector that the two cables connect to.
 By maintaining this parallelism, translation-only motion can be
 guaranteed, as will be shown in Section 7. This not only
 simplifies control of the manipulator, it also drastically reduces
 the complexity of the forward kinematics solution. Only three
 sets of the parallel cables are necessary to guarantee translation-
 only motion (much like the three sets of parallel links in the

Fig. 5. The contour crafting Cartesian cable robot (C^4 robot).Fig. 6. C^4 robot building a structure (concrete hose and storage tank shown).

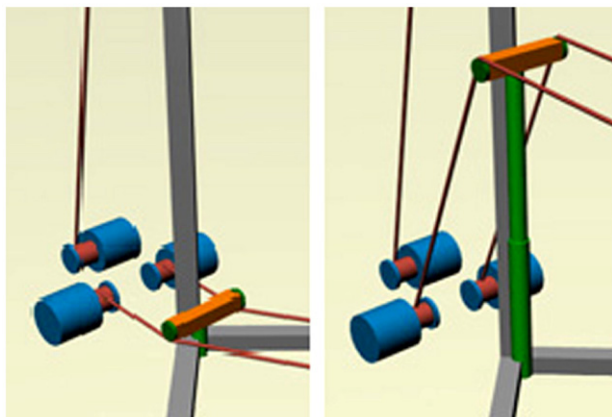


Fig. 7. Crossbar in lowered (left) and raised (right) configurations.

Delta robot [11]), however the addition of the fourth set increases the manipulator workspace.

Because the robot is fully-constrained, it can be engineered to have high stiffness relative to conventional manipulators and it can be designed to exert the required construction task forces and moments. Most fully-constrained cable robots have problems with cables interfering with each other and with surrounding objects. While the arrangement of the cables prevents interference between cables, it does not prevent interference with the building being constructed. In order to solve this problem, the horizontal crossbars on the frame are actuated vertically. Each crossbar can be independently linearly actuated along the vertical edge of the frame. This enables the manipulator to continuously reconfigure itself in order to avoid collisions between the lower cables and the building. Fig. 7 shows a close-up of the actuation of one of the crossbars. The actuation of the crossbars can be accomplished a number of ways, including via hydraulic pistons, gear/chain drives or cable drives. The actuation mechanism must also be properly shrouded in order to prevent jamming due to construction debris. The configuration of the cables allows for easy translation-only motion as well as easy forward and inverse position kinematics. The eight lower cables are grouped into pairs of parallel cables. Pure translational motion is accomplished by keeping the lengths of any two paired cables the same. In addition to simplifying the kinematic equations, this simplifies control of the manipulator.

4. System operation

Using this system to construct buildings will be accomplished as follows. The system is transported to the site with all elements of the system stowed. The system will actually be quite compact when stowed because the cables can be reeled in and the frame members will likely be constructed using trusses that can be easily assembled and disassembled. Once at the construction site, the frame is assembled, the cables are strung through the pulleys and are connected to the end-effector. The most critical step in the deployment of the system is properly leveling and anchoring the frame. It may be possible to add additional adjustable supports to the bottom of the frame that would allow it to be leveled.

When the system has been anchored, the robot must be calibrated. Due to space limitations a complete calibration routine cannot be discussed here. The construction material (concrete or a similar material) must be prepared and then pumped into the end-effector (as shown in Fig. 6). Assuming a proper foundation/footing for the structure is in place, the construction of the building can now begin. With the vertically-actuated crossbars all set to their lowest height, the end-effector is controlled to move along the desired trajectory for extruding the first layer of the structure's walls. The position of the end-effector is controlled by actuation of the 12 cables, where the length of any two paired parallel cables is kept the same. As the building is constructed a layer at a time, the height of the building will increase, making collisions between the lower cables and the building more likely. Thus after several layers have been completed each of the four actuated crossbars is raised (typically the same distance for each crossbar), allowing the robot to maintain full constraint of the end-effector while preventing any collisions between cables and the building (see Fig. 8). The entire structure is constructed in a layered fashion, with the crossbars being raised periodically to avoid collisions. The end-effector will also place structural elements such as header beams for overhangs such as windows or doorframes. This can be accomplished by mounting a serial robot arm to the end-effector, similar to what is proposed in [1] (see [1] for full details on this process).

Once the structure is completed, the C^4 robot system can be moved to a different work site to build another structure. If the next structure is to be nearby, it is not necessary to disassemble the construction system. Instead, one of the horizontal bottom members of the frame can be removed and the system can be moved (e.g. by the addition of wheels to the frame) away from the first structure and to the site of the second structure. Once all construction at the site is completed, the system can again be easily disassembled and stowed in a compact travel configuration.

5. C^4 robot kinematics

In this section we present some basic kinematic equations for control of the robot. The kinematic parameters of the robot are

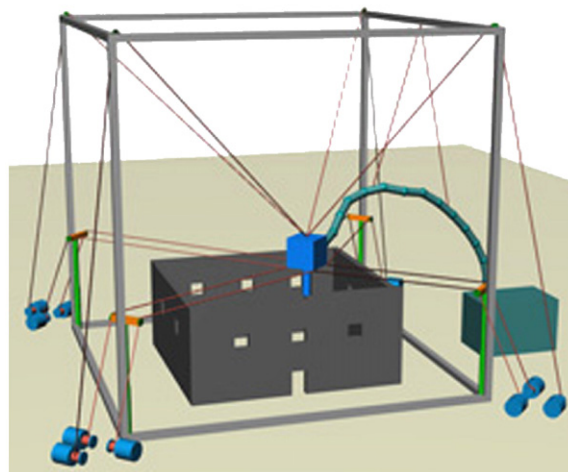


Fig. 8. C^4 robot building a structure with crossbars raised.

238 shown in Fig. 9. The frame is assumed to be a rectangular
 239 parallelepiped with sides of fixed length d_x, d_y, d_z . The base
 240 coordinate frame $\{B\}$ is attached as shown, fixed to the floor in
 241 the center of the XY plane. The end-effector is constructed of a
 242 rectangular parallelepiped with fixed side lengths p_x, p_y, p_z .
 243 Though this robot provides translational-only motion, the end-
 244 effector is rotated at assembly relative to the base frame. The
 245 nozzle frame $\{N\}$ is attached to the end of the extrusion nozzle;
 246 though $\{N\}$ translates relative to $\{B\}$, their orientation is
 247 constrained to be always the same. An additional frame $\{P\}$ is
 248 also parallel to $\{N\}$, but located at the geometric center of the
 249 end-effector rectangular parallelepiped (not shown in Fig. 9).

250 Due to the arrangement of the lower cables (the pairs of
 251 cables are parallel and the horizontal crossbar for each pair is
 252 parallel to the corresponding side of the end-effector), the
 253 orientation of the end-effector does not change, as will be
 254 proven in Section 7. The four pairs of lower cables of lengths
 255 have lengths L_1, L_2, L_3, L_4 , where for pair i each of the cables
 256 have length L_i . As shown in Fig. 9, the horizontal end-effector
 257 dimensions are p_x and p_y which are the same as the
 258 corresponding crossbar lengths. These are actuated to different
 259 heights along the vertical sides of the frame to variable heights
 260 h_1, h_2, h_3, h_4 . These heights can allow the cables to be free from
 261 interference with the house under construction. When viewed
 262 from above (as shown in Fig. 10) the crossbars and the end-
 263 effector are rotated 45° from the horizontal members of the
 264 frame. This angle was chosen to ensure workspace symmetry.

265 There are also four upper cables meeting in a point at the top
 266 center of the end-effector, with variable lengths L_5, L_6, L_7, L_8 .
 267 These cables are routed through fixed pulleys located at the
 268 upper vertices of the frame as shown in Figs. 5, 6 and 8.

269 5.1. Inverse position kinematics

270 For parallel robots such as this 12-cable-driven robot, the
 271 inverse position kinematics is generally straight-forward. The
 272 solution simply amounts to forming the known vectors between
 273 cable connection points and calculating their Euclidian norms to
 274 determine the associated required cable lengths. Due to space

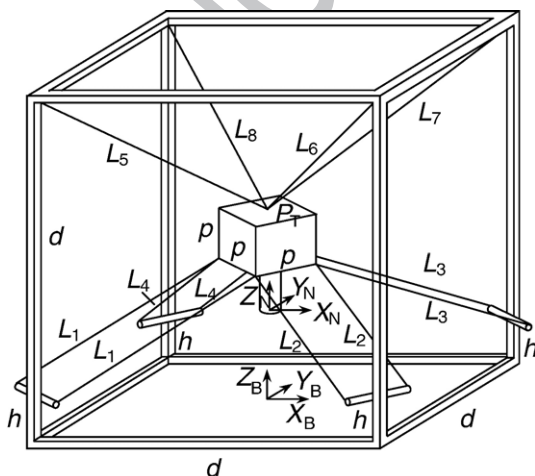


Fig. 9. Kinematic parameters of C^4 robot.

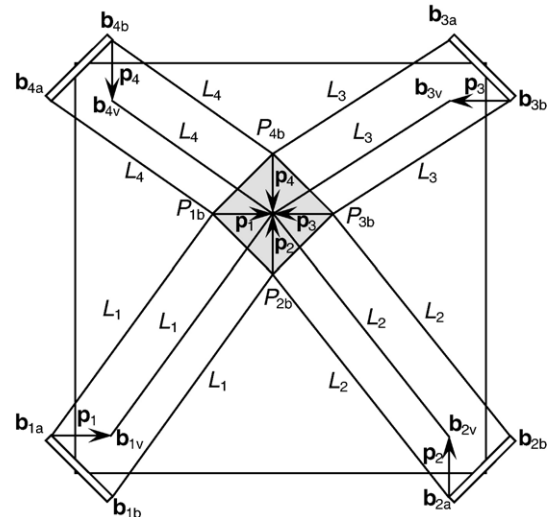


Fig. 10. Overhead view of C^4 robot with lower cables and virtual cables shown.

275 limitations and the simple nature of these equations they will not
 276 be detailed here.

277 5.2. Virtual cable concept

278 The forward kinematic equations will be described next.
 279 However, we will first discuss the concept of virtual cables,
 280 which will simplify the derivation of the forward kinematic
 281 equations.

282 We can simplify the kinematics problems by using a single
 283 control point P located at the origin of $\{P\}$, the geometric center
 284 of the end-effector rectangular parallelepiped. For the lower
 285 four parallel cable pairs we introduce four virtual cables, in
 286 place of the eight real drive cables as follows. From cable
 287 attachment points P_{ib} on the end-effector, draw vectors \mathbf{p}_i to P ,
 288 $i=1,2,3,4$ (see Fig. 10). Since the platform orientation is not
 289 changing, the orientations of all \mathbf{p}_i are constant. Now, from
 290 cable base points b_{ia} on the vertically-translating cable base
 291 supports, attach these same vectors \mathbf{p}_i to form virtual cable
 292 pulley points b_{iv} , as shown in Fig. 10. Connect a single virtual
 293 control cable between the two tips of these two vectors \mathbf{p}_i ,
 294 $i=1,2,3,4$. Then the length of these virtual cables is also L_i ,
 295 $i=1,2,3,4$, due to the parallelism. So the real kinematics prob-
 296 lems may be significantly simplified without loss of generality
 297 by controlling the four virtual cables L_i to translate P . Note that
 298 Fig. 10 shows the top view for clarity; all vectors shown are 3D,
 299 so their true lengths are not shown but rather the XY planar
 300 projections of their true lengths.

301 5.3. Forward position kinematics

302 The forward position kinematics problem is stated: given the
 303 twelve cable lengths L_i , calculate the desired contour-crafting
 304 nozzle position ${}^B\mathbf{P}_N = \{x_N y_N z_N\}^T$. In general, forward
 305 position kinematics for parallel (and cable-suspended) robots
 306 is very challenging, with multiple solutions. However, due to
 307 the virtual cable simplification discussed above, the current
 308 forward position kinematics solution is straight-forward and

309 may be solved in closed-form. The end-effector rectangular
 310 parallelepiped center P is simply the intersection of three given
 311 spheres. Using the lower virtual cables, we can choose any three
 312 of the four virtual cables $i=1,2,3,4$. Choosing the first three, the
 313 forward position kinematics solution for P is found from the
 314 intersection of the following three spheres, where each sphere is
 315 referred to as (vector center \mathbf{c} , scalar radius r):

$$316 \quad {}^B\mathbf{P}_P \rightarrow (\mathbf{b}_{1v}, L_1), (\mathbf{b}_{2v}, L_2), (\mathbf{b}_{3v}, L_3) \quad (1)$$

317 where points \mathbf{b}_{iv} are the virtual cable pulley points as shown in
 318 Fig. 10. A closed-form three spheres' intersection algorithm is
 319 presented in [13]. There are two solutions, from which the
 320 correct one may easily be selected by computer (the upper
 321 solution rather than the lower one, for the lower parallel cable
 322 pairs). There is the possibility of imaginary solutions only if the
 323 input data to the forward position problem is not consistent (i.e.
 324 sensing or modeling errors). There is an algorithmic singularity
 325 which may be avoided by proper choice of coordinate frames.
 326 Thus the forward position solution can be found by using only
 327 three virtual cables out of the 12 active cables. This is possible
 328 due to the translation-only motion of the robot. After forward
 329 position kinematics solution is found, the inverse position
 330 kinematics solution may be used to verify that the remaining
 331 cable lengths (unused in the forward position kinematics solu-
 332 tion) are correct.

333 There are many alternatives for solving the forward position
 334 kinematics solution of the 12-cable robot. For example, instead
 335 of intersecting spheres from 3 of the 4 lower virtual cables we
 336 can intersect 3 of the 4 upper real cables to find point P_T (on top
 337 of the end-effector). After we have point P from forward
 338 position kinematics with the lower virtual cables (or point P_T ,
 339 when using the upper cables) we can easily calculate the nozzle
 340 position.

341 In practice it may be possible to develop a forward position
 342 kinematics solution using all 8 cable lengths simultaneously (4
 343 upper real and 4 lower virtual) to reduce errors in the case of
 344 real-world sensing of the cable lengths.

345 6. C^4 robot statics

346 This section presents statics modeling for the 12-cable
 347 robot. For static equilibrium the sum of external forces and
 348 moments exerted on the end-effector by the cables must equal
 349 the resultant external wrench exerted on the environment.
 350 Because of the analogous relationship between cable robots
 351 and parallel robots, the well-known Jacobian relationship can
 352 be used to express the static equations. Let \mathbf{F}_R and \mathbf{M}_R be the
 353 resultant force and moment, respectively, applied by the end-
 354 effector to its surroundings (due to interaction forces and
 355 moments in the contour crafting process), expressed at point P
 356 in frame $\{P\}$. Position vector ${}^P\mathbf{P}_{CG}$ gives the location of the
 357 CG relative to P . In practice ${}^P\mathbf{P}_{CG}$ can be non-zero and even
 358 changing during the process as material is pumped in and
 359 extruded out. Let $\hat{\mathbf{L}}_i$ be the unit vector along cable i , directed
 360 away from the end-effector. Let \mathbf{p}_i be the position vector from
 361 the origin of $\{P\}$ to the point of connection of the i th cable to

the end-effector. Then the wrench \mathbf{W}_R applied by the end- 362
 effector on its surroundings is related to the vector of cable 363
 tensions $\mathbf{t}=(t_{1a} t_{1b} t_{2a} t_{2b} \dots t_{4b} t_5 t_6 t_7 t_8)^T$ according to: 364

$$365 \quad \mathbf{A}\mathbf{t} + \left\{ \begin{matrix} m\mathbf{g} \\ {}^P\mathbf{P}_{CG} \times m\mathbf{g} \end{matrix} \right\} = \mathbf{W}_R = \left\{ \begin{matrix} \mathbf{F}_R \\ \mathbf{M}_R \end{matrix} \right\} \quad (2) \quad 365$$

where the statics Jacobian \mathbf{A} (expressed in $\{B\}$ coordinates) is: 366

$$367 \quad \mathbf{A} = \begin{bmatrix} \hat{\mathbf{L}}_{1a} & \hat{\mathbf{L}}_{1b} & \hat{\mathbf{L}}_{2a} & \dots & \hat{\mathbf{L}}_7 & \hat{\mathbf{L}}_8 \\ \mathbf{p}_{1a} \times \hat{\mathbf{L}}_{1a} & \mathbf{p}_{1b} \times \hat{\mathbf{L}}_{1b} & \mathbf{p}_{2a} \times \hat{\mathbf{L}}_{2a} & \dots & \mathbf{p}_7 \times \hat{\mathbf{L}}_7 & \mathbf{p}_8 \times \hat{\mathbf{L}}_8 \end{bmatrix} \quad (3) \quad 367$$

The gravity vector is $\mathbf{g}=\{0 \ 0 \ -g\}^T$ and the end-effector mass 369
 is m . The forward statics solution is Eq. (2). The inverse statics 370
 problem is more useful, calculating the required cable tensions \mathbf{t} 371
 given the wrench \mathbf{W}_R . The statics Eq. (2) can be inverted in an 372
 attempt to support the end-effector weight while maintaining all 373
 cable tensions positive. 374

For cable robots with actuation redundancy, Eq. (2) is 375
 underconstrained which means that there are infinite solutions 376
 to the cable tension vector \mathbf{t} to exert the required Cartesian 377
 wrench \mathbf{W}_R . To invert Eq. (2) we adapt the well-known 378
 particular and homogeneous solution from resolved-rate control 379
 of kinematically-redundant serial manipulators: 380

$$381 \quad \mathbf{t} = \mathbf{A}^+ \mathbf{W}_R + (\mathbf{I} - \mathbf{A}^+ \mathbf{A}) \mathbf{z} \quad (4) \quad 381$$

where for the 12-cable robot \mathbf{I} is the 12×12 identity matrix, \mathbf{z} is 382
 an arbitrary 12-vector, and $\mathbf{A}^+ = \mathbf{A}^T (\mathbf{A} \mathbf{A}^T)^{-1}$ is the 12×6 383
 underconstrained Moore–Penrose pseudoinverse of \mathbf{A} . The first 384
 term of Eq. (4) is the particular solution $\mathbf{t}_p = \mathbf{A}^+ \mathbf{W}_R$ to achieve 385
 the desired wrench, and the second term is the homogeneous 386
 solution $\mathbf{t}_h = (\mathbf{I} - \mathbf{A}^+ \mathbf{A}) \mathbf{z}$ that projects \mathbf{z} into the null space of \mathbf{A} . 387
 So in principle the second term of Eq. (4) may be used to 388
 increase cable tensions until all are positive, while not changing 389
 the required Cartesian wrench. To implement Eq. (4) we use 390
 MATLAB function *lsqnonneg*, which solves the least-squares 391
 problem for Eq. (2) subject to all non-negative cable tensions. 392

393 7. Translation-only motion of the robot

394 As described earlier, the C^4 robot produces translation-only 394
 motion of the end-effector if the lengths of any two paired 395
 cables remain equal to each other. 396

Proof. Consider three pairs of lower cables. For this proof we 397
 will consider cables $1a$, $1b$, $2a$, $2b$, $3a$ and $3b$ as shown in 398
 Fig. 10 (note that the subscripts a and b are not shown in the 399
 figure, but are simply used here to denote each of the two 400
 cables in a pair). Let us construct a Jacobian matrix relating the 401
 rate at which the cables are reeled in to the resulting twist 402
 (linear and angular velocity) of the end-effector: 403

$$404 \quad \dot{\mathbf{q}} = \mathbf{J} \begin{pmatrix} \mathbf{v} \\ \boldsymbol{\omega} \end{pmatrix} \quad (5) \quad 404$$

where $\dot{\mathbf{q}}=(\dot{q}_{1a} \dot{q}_{1b} \dot{q}_{2a} \dot{q}_{2b} \dot{q}_{3a} \dot{q}_{3b})^T$ is the vector of cable rates, 405
 \mathbf{v} is the linear velocity of the end-effector (expressed in $\{B\}$), $\boldsymbol{\omega}$ 406

407 is the angular velocity of the end-effector (expressed in $\{B\}$)
408 and

$$409 \mathbf{J} = \begin{bmatrix} \hat{\mathbf{L}}_{1a} & \hat{\mathbf{L}}_{1b} & \hat{\mathbf{L}}_{2a} & \hat{\mathbf{L}}_{2b} & \hat{\mathbf{L}}_{3a} & \hat{\mathbf{L}}_{3b} \\ \mathbf{p}_{1a} \times \hat{\mathbf{L}}_{1a} & \mathbf{p}_{1b} \times \hat{\mathbf{L}}_{1b} & \mathbf{p}_{2a} \times \hat{\mathbf{L}}_{2a} & \mathbf{p}_{2b} \times \hat{\mathbf{L}}_{2b} & \mathbf{p}_{3a} \times \hat{\mathbf{L}}_{3a} & \mathbf{p}_{3b} \times \hat{\mathbf{L}}_{3b} \end{bmatrix}^T \quad (6)$$

410
411 Note that due to the parallelism of the cables $\hat{\mathbf{L}}_{ia} = \hat{\mathbf{L}}_{ib}$ for
412 $i = 1, 2, 3$. If we assume the manipulator starts from a pose where
413 cables ia and ib have the same length ($L_{ia} = L_{ib}$; $i = 1, 2, 3$) and
414 constrain the actuation of the cables such that $L_{ia} = L_{ib}$ for any
415 motion, then we can differentiate this relation to get

$$416 \dot{q}_{ia} = \dot{q}_{ib}, i = 1, 2, 3 \quad (7)$$

418 Consider the case where we actuate the lengths of only
419 cables $1a$ and $1b$ while holding the other lengths fixed: $\dot{\mathbf{q}}_1 =$
420 $(\dot{q}_1 \dot{q}_1 0 0 0 0)^T$. Then

$$421 \dot{\mathbf{q}}_1 = \mathbf{J} \begin{pmatrix} \mathbf{v}_1 \\ \omega_1 \end{pmatrix}. \quad (8)$$

422
423 We anticipate a solution for $(\mathbf{v}_1 \ \omega_1)^T$ that results only in
424 translation, so we assume for now that $\omega_1 = \bar{\mathbf{0}} = (0 \ 0 \ 0)^T$. Eq. (8)
425 represents a set of six equations. We examine the four equations
426 resulting from the bottom four rows of \mathbf{J} :

$$427 0 = [(\hat{\mathbf{L}}_{2a})^T (\mathbf{p}_{2a} \times \hat{\mathbf{L}}_{2a})^T] \begin{pmatrix} \mathbf{v}_1 \\ \bar{\mathbf{0}} \end{pmatrix} \quad (9)$$

$$429 0 = [(\hat{\mathbf{L}}_{2b})^T (\mathbf{p}_{2b} \times \hat{\mathbf{L}}_{2b})^T] \begin{pmatrix} \mathbf{v}_1 \\ \bar{\mathbf{0}} \end{pmatrix} \quad (10)$$

$$431 0 = [(\hat{\mathbf{L}}_{3a})^T (\mathbf{p}_{3a} \times \hat{\mathbf{L}}_{3a})^T] \begin{pmatrix} \mathbf{v}_1 \\ \bar{\mathbf{0}} \end{pmatrix} \quad (11)$$

$$433 0 = [(\hat{\mathbf{L}}_{3b})^T (\mathbf{p}_{3b} \times \hat{\mathbf{L}}_{3b})^T] \begin{pmatrix} \mathbf{v}_1 \\ \bar{\mathbf{0}} \end{pmatrix}. \quad (12)$$

434
435 Using the fact that $\hat{\mathbf{L}}_{ia} = \hat{\mathbf{L}}_{ib}$ for $i = 1, 2, 3$, it is straightforward
436 to see that if $(\hat{\mathbf{L}}_{2a})^T \mathbf{v}_1 = 0$ and $(\hat{\mathbf{L}}_{3a})^T \mathbf{v}_1 = 0$ (i.e. \mathbf{v}_1 is
437 perpendicular to both $\hat{\mathbf{L}}_{2a}$ and $\hat{\mathbf{L}}_{3a}$) then Eqs. (9)–(12) are
438 satisfied. If we now examine the first two equations (resulting
439 from the first two rows of \mathbf{J}), and use the fact that $\hat{\mathbf{L}}_{1a} = \hat{\mathbf{L}}_{1b}$ we
440 get two identical equations:

$$441 \dot{q}_1 = (\hat{\mathbf{L}}_{1a})^T \mathbf{v}_1. \quad (13)$$

443 Thus the $(\mathbf{v}_1 \ \omega_1)^T$ that solve Eq. (8) can be found, where
444 $\omega_1 = \bar{\mathbf{0}} = (0 \ 0 \ 0)^T$, the direction of \mathbf{v}_1 is found as perpendicular to
445 both $\hat{\mathbf{L}}_{2a}$ and $\hat{\mathbf{L}}_{3a}$, and the magnitude of \mathbf{v}_1 is then found from
446 Eq. (13). Because \mathbf{J} is a square non-singular matrix, this
447 solution is a unique solution of Eq. (8), and thus our assumption
448 of $\omega_1 = \bar{\mathbf{0}} = (0 \ 0 \ 0)^T$ was correct.

449 Similar analyses can be performed to determine the twist of
450 the end-effector for actuation of only the second set of cables
451 (where $\dot{\mathbf{q}}_2 = (0 \ 0 \ \dot{q}_2 \ \dot{q}_2 \ 0 \ 0)^T$) and actuation of only the third set
452 of cables (where $\dot{\mathbf{q}}_3 = (0 \ 0 \ 0 \ 0 \ \dot{q}_3 \ \dot{q}_3)^T$). These analyses also
453 result in motion of the end-effector where $\omega_2 = \omega_3 = \bar{\mathbf{0}} = (0 \ 0 \ 0)^T$.

Now due to the linearity of Eq. (5), any solution of Eq. (5) where
454 $\dot{q}_{ia} = \dot{q}_{ib}$, $i = 1, 2, 3$ can be found as a superposition of the
455 three solutions to the cases where only one pair of cables is
456 actuated at a time. Each of these cases has been shown to result
457 in $\omega = \bar{\mathbf{0}}$, thus we can conclude that for any arbitrary allowed
458 actuation of the cables $\omega = \bar{\mathbf{0}}$. We can now integrate this result
459 and conclude that if parallelism of the cables is maintained, the
460 matrix \mathbf{J} is non-singular, and the cable actuation satisfies
461 Eq. (7), then the manipulator will not rotate and undergoes
462 translation-only motion. \square 463

464 Note that because of the geometry of the manipulator, trans-
465 lation of the end-effector guarantees that the cables remain
466 parallel, thus that assumption is valid. In addition, throughout
467 the workspace of the manipulator (which is found in Section 8)
468 our assumption of a non-singular \mathbf{J} is valid as well.

8. C^4 robot workspace 469

470 One of the key characteristics of this robot is its workspace.
471 Specifically, we desire for the manipulator to reach and be able
472 to perform CC tasks at any x – y – z position encompassed by the
473 frame of the robot. Formally, we will define the workspace of
474 the C^4 robot as the set of all x – y – z positions that the point P
475 can attain (in $\{B\}$) while maintaining full constraint of the end-
476 effector and being able to exert a specified set of forces and
477 moments on its surroundings with all non-negative cable ten-
478 sions and without any of the cables exceeding their upper
479 tension limits. This has also been termed the “wrench-feasible
480 workspace” of a cable robot [14].

481 In order to investigate the workspace of this robot, an example
482 geometry was chosen and the workspace generated numerically
483 using MATLAB. While this geometry is not necessarily exactly
484 what will be used in practice, it is sufficiently “generic” that the
485 resulting trends are expected to generalize. This example
486 geometry consists of a 1 m cube end-effector manipulated within
487 a 50 m cube frame. Due to the end-effector dimensions, each of
488 the horizontal crossbars is 1 m wide. The end-effector has a mass
489 of 1000 N and the maximum allowable tension in a cable is 10 kN.
490 The space within the robot’s frame is discretized into 2 m cubes.
491 In addition to supporting the weight of the end-effector, at each
492 position the robot is required to exert a force of ± 450 N in the x , y
493 and z directions and a moment of ± 200 N m about the x , y and z
494 axes. For each of these loading conditions the tensions in the
495 cables are determined. Recall that the statics equations of the
496 manipulator are underdetermined, thus the cable tensions cannot
497 be determined uniquely. To resolve this we use MATLAB func-
498 tion *lsqnonneg*, which solves the least-squares problem for Eq.
499 (2) subject to all non-negative cable tensions. The maximum
500 single cable tension is determined for each individual loading
501 condition, and then the overall maximum tension (the maximum
502 single cable tension considering all of the loading conditions) is
503 determined for the pose.

504 **Figs. 11–17** show the results of this simulation. **Fig. 11** shows
505 the workspace of the C^4 robot with the horizontal crossbars all
506 set to a height of 0 m. Every position that is reachable with
507 acceptable cable tensions ($0 \leq t_i \leq 10$ kN) is represented by a
508 colored box, with the color of the box representing the overall

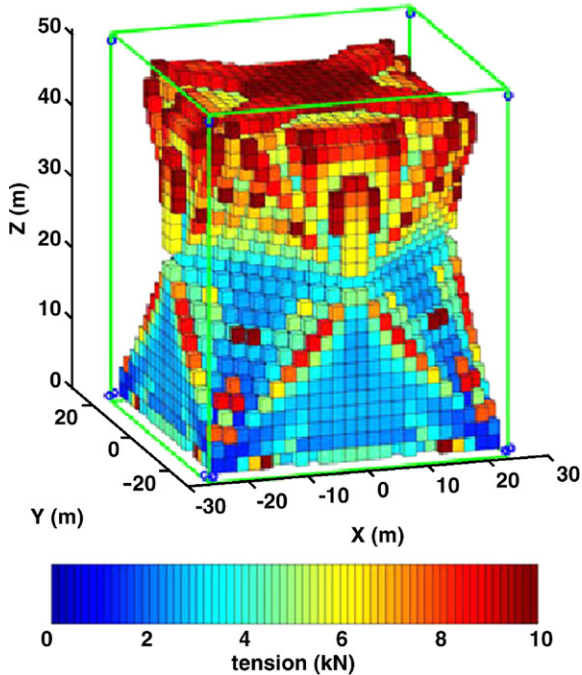


Fig. 11. Workspace of C^4 Robot with 1 m cube end-effector, colors indicate overall maximum cable tension. (For interpretation of the references to colour in this figure legend, the reader is referred to the web version of this article.)

509 maximum tension for the pose. The color key for Figs. 11–17 is
 510 given in Fig. 11. The robot's frame is represented by the green
 511 cube surrounding the workspace and the locations of the twelve
 512 pulleys (one for each of the twelve cables) are represented by
 513 blue circles. In Fig. 11 we can see that the workspace of the robot
 514 is quite large, filling a large majority of the volume within the
 515 frame. Due to the symmetry of the robot geometry the workspace
 516 is also symmetric.

517 The workspace of Fig. 11 is sliced along the $x=0$ plane and
 518 the $y=0$ plane, resulting in a quarter section of the workspace
 519 shown in Fig. 12. This section reveals that the interior of the

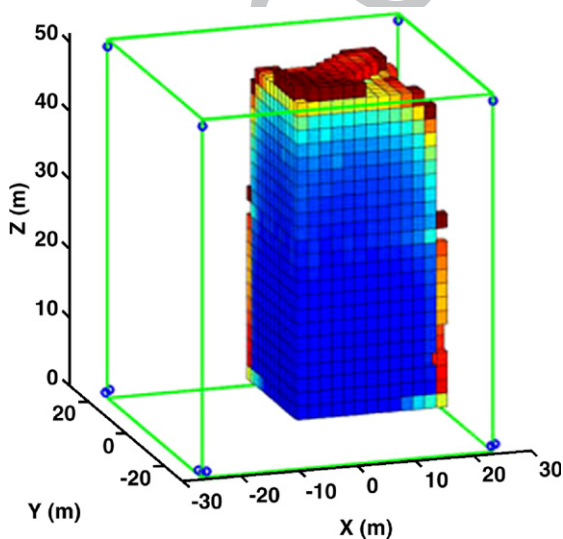


Fig. 12. Quarter section of workspace of Fig. 11.

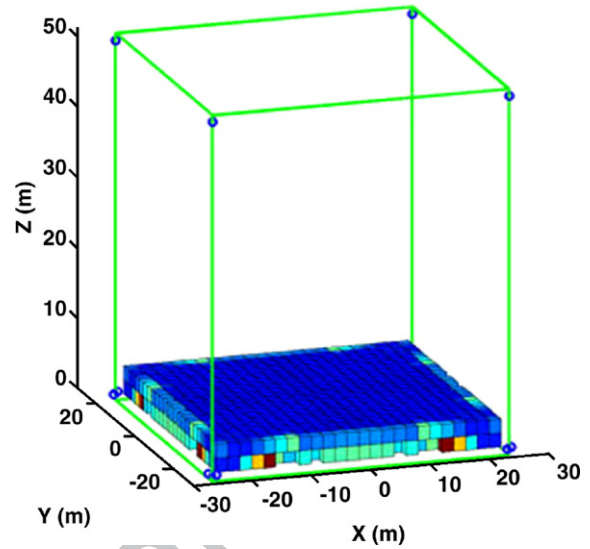


Fig. 13. Section of workspace of Fig. 11 below $Z=3$ m.

workspace has generally low tensions in the cables, which is
 520 desirable. Because the manipulator will operate low in this
 521 workspace (i.e. once the structure under construction is built up
 522 a few meters, the crossbars will be raised to avoid interference)
 523 we are particularly interested in the structure of the workspace
 524 near its bottom. Accordingly, consider Fig. 13, which is the
 525 workspace of Fig. 11 sliced along the $z=3$ m plane. Again we
 526 can see that the interior of the workspace has generally low
 527 tensions, with higher tensions only occurring near the edges of
 528 the workspace. This plot indicates that a robot of this geometry
 529 could safely construct a structure with a foundation that is
 530 contained within a roughly 44×44 m area.
 531

As the construction of the building continues, the crossbars
 532 will need to be raised in order to avoid interference of the cables
 533 with the building under construction. The crossbars need only
 534 be raised a few meters at a time. As a representative example the
 535

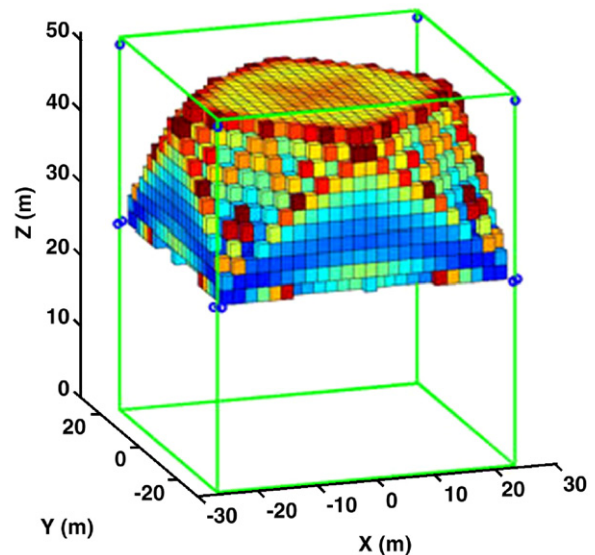
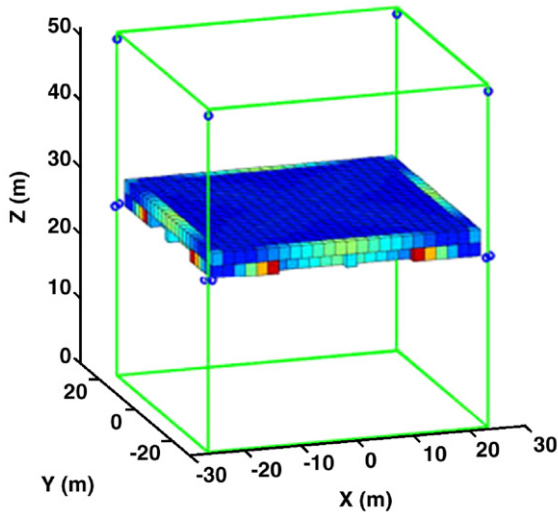
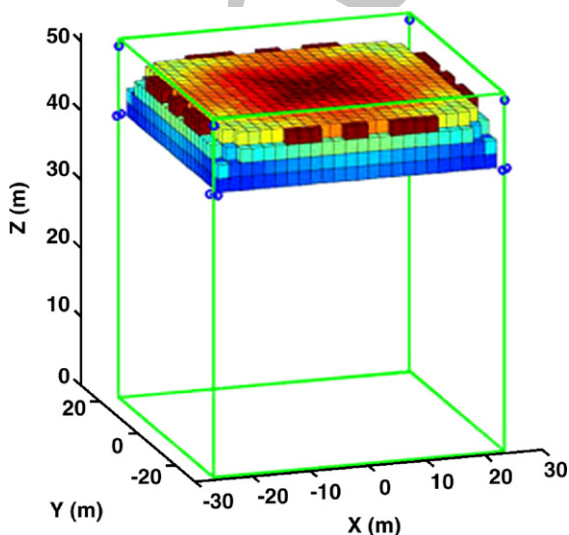
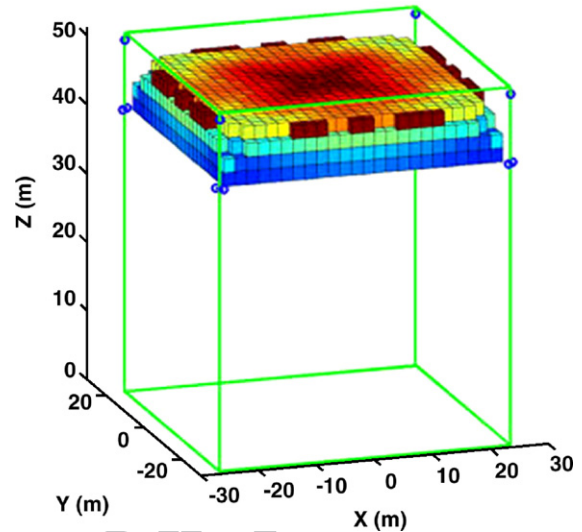


Fig. 14. Workspace of C^4 robot with crossbars moved to $Z=25$ m.

Fig. 15. Section of workspace of Fig. 14 below $Z=28$ m.

536 workspace of the robot is shown in Fig. 14 with the horizontal
 537 crossbars all set to a height of 25 m. Again the workspace is
 538 fairly large, filling the majority of the space from $z=25$ to 50 m
 539 in the frame. More importantly, the workspace is wide in the
 540 vicinity of $z=25$ m, where the end-effector will be operating
 541 during this stage of construction. This can be seen in Fig. 15,
 542 where the workspace of Fig. 14 is sliced along the $z=28$ m
 543 plane. Again we can see that the interior of the workspace has
 544 generally low tensions, with higher tensions only occurring near
 545 the edges of the workspace. In addition, the usable area of this
 546 portion of the workspace is still approximately 44×44 m.

547 Lastly, we consider the workspace of the robot with the
 548 crossbars raised to 40 m, which is near the maximum expected
 549 height for the crossbars. The resulting workspace of the robot is
 550 shown in Fig. 16. The workspace is not particularly large,
 551 however the workspace is very wide in the vicinity of $z=40$ m,
 552 where the end-effector will be operating during this stage of
 553 construction. This can be seen in Fig. 17, where the workspace

Fig. 16. Workspace of C^4 robot with crossbars moved to $Z=40$ m.Fig. 17. Section of workspace of Fig. 16 below $Z=43$ m.

of Fig. 16 is sliced along the $z=43$ m plane. The interior of this
 554 section has larger tensions than those seen in Figs. 13 and 15,
 555 but none higher than 4 kN. Given the usable area of this portion
 556 of the workspace, it appears that the maximum size building that
 557 can be constructed with this robot using our example geometry
 558 is approximately $44 \times 44 \times 40$ m, which is very effective con-
 559 sidering the 50 m cube frame.
 560

9. Cost and productivity analysis

561
 562 Analysis of a typical construction operation performed with
 563 conventional methods will yield information on costs and
 564 productivity rates as a basis for comparison with the proposed
 565 CC operation. Placing and vibrating concrete is a work item
 566 shown in standard cost guides [15]. In particular, the item to be
 567 estimated consists of placing and vibrating structural concrete
 568 for a 12" (0.305 m) thick wall, considering three situations:
 569 direct chute, pumped, and with crane and bucket. The daily
 570 output, costs and crews associated with these tasks are listed in
 571 Table 1. Costs include labor, equipment, overhead and profit
 572 average values from contractors in the United States.

573 Table 1 indicates an average operation cost of about US\$40/
 574 m^3 and a productivity of $77 m^3/day$. It also shows the crew
 575 composition for each task, which at its simplest situation denotes
 576 the presence of one foreman, four laborers and one cement
 577 finisher. The other situations feature a more labor-intensive
 578 environment.

579 The determination of costs and productivity outputs for the
 580 C^4 robot operation will be based on the hypothetical con-
 581 struction of a 20 m wide, 12" (0.305 m) thick, 4 m tall foun-
 582 dation wall. This workspace dimension will allow the robot
 583 manipulator to fully exert CC tasks while reaching wall areas
 584 with the end-effector, as explained in the previous section (" C^4
 585 robot workspace"). Although conventional concrete will not be
 586 the most suitable material for CC tasks due to expected prob-
 587 lems with aggregate congestion in the nozzle, compacting dif-
 588 ficulties, spacing limitations due to rebar and formwork

589 installation and other constraints due to the nature of this tra-
590 ditionally manual task, other materials such as self-compacted
591 concrete will expedite concrete compaction while maintaining
592 the quality of the structure [16]. On the other hand, extruded
593 concrete addresses the formwork, aggregate and rebar issue by
594 using fibers that improve the cohesion of the concrete mix [17].

595 In the case study of the 20 m wide, 12" (0.305 m) thick, 4 m
596 tall foundation wall, the C⁴ robot operation will place 12" wide
597 (0.305 m), 2" tall (5.08 cm) layers at a conservative speed of
598 1 km/h, finishing one layer in approximately 0.02 h. The CC
599 operation for the entire foundation wall will take approximately
600 1.57 h, which will be rounded to 2 h due to manipulator set up,
601 height adjustment and contingencies, about 25% of the working
602 time. The CC productivity for the entire foundation wall
603 operation will yield a value of approximately 12.2 m³/h, or
604 97.6 m³/day, considering an 8-h working day. For the
605 determination of costs, a combination of concrete pump costs
606 and manipulator operational costs will be used for this endeavor.
607 Also, a labor foreman, responsible for overseeing the operation
608 and monitoring the concrete supply, will be included in the
609 estimate. The manipulator operational costs are related to the
610 energy source used for powering the unit (e.g., grid, compressor,
611 etc.). An estimated daily amount can be extrapolated from
612 equivalent design elements at the bench scale level [15]: one
613 compressor (US\$120), one 25-ton crane (US\$651), one concrete
614 conveyor (US\$152), one small concrete pump (US\$700) and
615 one labor foreman (\$185). This yields a total of US\$1808/day.
616 Cost data for the manipulator control operations, including
617 electronic instrumentation and tension mechanisms are still
618 uncertain. However, a preliminary estimate of US\$2,000/day
619 will be used for comparison. Using the productivity of 97.6 m³/
620 day estimated earlier, the cost per m³ is estimated to be about US
621 \$39. This estimate is greater than the current method of direct
622 chute (US\$24) and the same as the pumping method (US\$39),
623 but is lower than the labor-intensive operation with crane and
624 bucket (US\$57). In summary, Table 2 shows the cost and
625 productivity comparison for conventional vs. CC construction,
626 for the case illustrated.

627 The conventional task depicted in Table 2 corresponds to the
628 average values of Table 1, but including the crew for the direct
629 chute, which the least labor-intensive. The CC task presents a

Table 2
Cost and productivity comparison

Task	Crew	Daily output (m ³ /day)	Cost (US\$/m ³)
Conventional	1 foreman, 4 laborers, 1 cement finisher	77	40
CC	1 foreman	98	39

higher daily output when compared to the conventional task
(27% greater). The CC cost is very similar to the conventional
operation. Although the values used for the robot manipulator
are approximated to its conversion from a bench scale opera-
tion, these values are still conservative. Furthermore, there are
additional costs that could be saved in the CC operation. Acci-
dent costs, safety training, and labor burden are considerable
costs that are not estimated upfront. CC is a more economical
alternative, since these costs are not as significant as in the
conventional concrete operation task.

10. Conclusions and future work

This article has presented a new cable robot, the C⁴ robot,
designed for use in a contour crafting system. It combines
several novel features, including a geometry that permits
translation-only motion and highly simplified kinematic equa-
tions, and the use of actuated cable mounts that allow on-line
reconfiguration of the cable robot to eliminate cable interference
while maintaining full constraint of the end-effector. This system
can be engineered to provide the ability to contour-craft large
structures with the potential for being less expensive and more
portable than existing robot concepts for contour crafting.

The forward and inverse position kinematics solutions were
discussed, which incorporated the concept of virtual cables in
order to simplify the forward position kinematics. The static
equations were presented, including a discussion of how the
redundancy of the manipulator can be used to maintain non-
negative tensions in all cables. The manipulator's workspace
was investigated for an example geometry, including calcula-
tion of the maximum cable tension for a variety of loading
conditions. The workspace was determined to be potentially
very large, with low maximum cable tensions for nearly all
positions. Based on this workspace analysis, it was concluded
that the frame of the robot only needs to be slightly larger than
the building being constructed. Lastly, an initial cost and
productivity analysis was presented, which must be updated as
this concept and the construction industry progresses.

Future plans for manipulator development include construct-
ing a small-scale prototype, detailed mechanical design of the
system components, and development of calibration routines and
automated controller. Additional work is also planned on im-
proved construction materials and extrusion/troweling tooling.

References

- [1] B. Khoshnevis, Automated construction by contour crafting — related
robotics and information technologies, *Journal of Automation in
Construction — Special Issue: The Best of ISARC 2002* 13 (1) (January
2004) 5–19.

Table 1
Cost and productivity data for placing and vibrating 12" wall concrete (adapted
from [15])

Task	Crew	Daily output (m ³ /day)	Cost (US\$/m ³)
Direct chute	1 foreman, 4 laborers, 1 cement finisher	77	24
Pumped	1 foreman, 5 laborers, 1 cement finisher, 1 equipment operator	85	39
With crane and bucket	1 foreman, 5 laborers, 1 cement finisher, 1 equipment operator, 1 equipment oiler	69	57
Average		77	40

- 676 [2] B. Khoshnevis, R. Russel, H. Kwon, S. Bukkapatnam, Crafting large
677 prototypes, IEEE Robotics & Automation Magazine (September 2001)
678 33–42. 699
- 679 [3] S. Kawamura, W. Choe, S. Tanaka, S. Pandian, Development of an
680 ultrahigh speed robot FALCON using wire drive system, Proceedings of
681 the 1993 IEEE International Conference on Robotics and Automation,
682 vol. 1, May 1995, pp. 215–220, Nagoya, Japan. 700
- 683 [4] J. Albus, R. Bostelman, N. Dagalakis, The NIST RoboCrane, Journal of
684 National Institute of Standards and Technology 97 (3) (May–June 1992). 701
- 685 [5] J.J. Gorman, K.W. Jablow, D.J. Cannon, The cable array robot: theory
686 and experiment, Proceedings of the 2001 IEEE International Conference
687 on Robotics and Automation, 2001, pp. 2804–2810. 702
- 688 [6] R.L. Williams II, J. Albus, R. Bostelman, Self-contained automated
689 construction deposition system, Automation in Construction 13 (2004)
690 393–407. 703
- 691 [7] C. Bonivento, A. Eusebi, C. Melchiorri, M. Montanari, G. Vassura,
692 WireMan: a portable wire manipulator for touch-rendering of bas-relief
693 virtual surfaces, Proceedings of the 1997 International Conference on
694 Advanced Robotics (ICAR 97), 1997, pp. 13–18. 704
- 695 [8] R.L. Williams II, Cable-suspended haptic interface, International Journal
696 of Virtual Reality 3 (3) (1998) 13–21. 705
- 697 [9] K. Maeda, S. Tadokoro, T. Takamori, M. Hiller, R. Verhoeven, On design
698 of a redundant wire-driven parallel robot WARP manipulator, Proceedings
721 of the 1999 IEEE International Conference on Robotics and Automation,
(Detroit, Michigan), May 1999, pp. 895–900. 706
- [10] S. Tadokoro, Y. Mura, M. Hiller, R. Murata, H. Kohkawa, T. Matsushima,
A motion base with 6-DOF by parallel cable drive architecture, IEEE/
ASME Transactions on Mechatronics 7 (June 2002) 115–123. 707
- [11] R. Clavel, Delta: a fast robot with parallel geometry, Proceedings of the
18th International Symposium on Industrial Robot, 1988. 708
- [12] P. Bosscher, R.L. Williams II, M. Tummino, A concept for rapidly-
deployable cable robot search and rescue systems, Proceedings of the 2005
ASME DETC/CIE Conferences, (Long Beach, California), DETC2005-
84324, September 2005. 709
- [13] R.L. Williams II, J.S. Albus, R.V. Bostelman, 3D cable-based Cartesian
metrology system, Journal of Robotic Systems 21 (5) (2004) 237–257. 710
- [14] P. Bosscher, 2004. “Disturbance robustness measures and wrench-feasible
workspace generation techniques for cable-driven robots”. PhD thesis,
Georgia Institute of Technology, Atlanta, GA, November. 711
- [15] R.S. Means, Open shop building construction cost data, 22nd Annual
Edition, 03300, Cast-in-Place Concrete, RS Means CMD Group, 2006. 712
- [16] H. Okamura, M. Ouchi, Self-compacting concrete, Journal of Advanced
Concrete Technology 1 (15) (2003) 5–15. 713
- [17] V. Li, Large volume, high-performance applications of fibers in civil
engineering, Journal of Applied Polymer Science 83 (3) (2001) 660–686. 714
- 715
716
717
718
719
720